

# PROBABILISTIC ASSESSMENT OF EARTHQUAKE-INDUCED SLIDING DISPLACEMENTS OF NATURAL SLOPES

Ellen M. Rathje<sup>1</sup> and Gokhan Saygili<sup>2</sup>

## SUMMARY

The evaluation of earthquake-induced landslides in natural slopes is often based on an estimate of the permanent sliding displacement due to earthquake shaking. Current procedures for estimating sliding displacement do not rigorously account for the significant uncertainties present in the analysis. This paper presents a probabilistic framework for computing the annual rate of exceedance of different levels of displacement such that a hazard curve for sliding displacement can be developed. The analysis incorporates the uncertainties in the prediction of earthquake ground shaking, in the prediction of sliding displacement, and in the assessment of soil properties. Predictive models for sliding displacement that are appropriate for the probabilistic framework are presented. These models include a scalar model that predicts sliding displacement in terms of a single ground motion parameter (peak ground acceleration) and the earthquake magnitude, as well as a vector model that incorporates two ground motion parameters (peak ground acceleration and peak ground velocity). The addition of a second ground motion parameter results in a significant reduction in the standard deviation of the sliding displacement prediction. Comparisons are made between displacement hazard curves developed from the current scalar and vector models and previously developed scalar models that do not include earthquake magnitude. Additionally, an approximation to the vector hazard assessment is presented and compared with the rigorous vector approach. Finally, the inclusion of the soil property uncertainty is shown to increase the mean hazard at a site.

## INTRODUCTION

Earthquake-induced sliding displacements are commonly used to assess the seismic performance of slopes. These displacements represent the cumulative, downslope movement of a sliding block due to earthquake shaking. While the sliding block model is a simplified representation of the field conditions, the displacements predicted from this model have been shown to be a useful index of seismic performance [e.g., 1, 2].

The sliding block model can be further simplified by assuming the sliding mass to be rigid and ignoring its dynamic response. While this assumption is not valid for deeper sliding masses, it generally is applicable to natural slopes that commonly fail on shallow failure planes [3]. The rigid block model has been the basis of earthquake-induced landslide hazard maps in California [4].

Two parameters are required to compute the earthquake-induced sliding displacement of a slope: the yield acceleration ( $k_y$ ) for the slope and the acceleration-time history of the ground ( $a$ ). The yield acceleration represents the horizontal acceleration (in units of  $g$ , the acceleration of gravity) that results in a factor of safety of 1.0 and initiates sliding in the slope.  $K_y$  can be derived from an infinite slope approximation of a shallow failure surface, along with the geometry and shear strength parameters of the slope (Figure 1):

$$k_y = \frac{(FS - 1) \cdot g}{(\cos \alpha \cdot \tan \phi + 1 / \tan \alpha)} \quad (1)$$

$$FS = \frac{c'}{\gamma \cdot t \cdot \sin \alpha} + \frac{\tan \phi'}{\tan \alpha} - \frac{\gamma_w \cdot m \cdot \tan \phi'}{\gamma \cdot \tan \alpha} \quad (2)$$

where  $FS$  = static factor of safety;  
 $\alpha$  = slope angle;  
 $c'$  = effective cohesion;  
 $\phi'$  = effective friction angle;  
 $t$  = slope normal thickness of failure surface;  
 $m$  = percentage of failure thickness that is saturated;  
 $\gamma$  = unit weight of soil; and  
 $\gamma_w$  = unit weight of water.

To compute sliding displacement ( $D$ ) for a given acceleration-time history, a sliding episode begins when  $a > k_y$  and continues until the velocity of the sliding block and ground again coincide. The relative velocity between the rigid block and the ground is integrated with respect to time to calculate the sliding displacement for each sliding episode and the sum of the displacements for each sliding episode represents the cumulative sliding displacement for the given acceleration-time history.

<sup>1</sup> J. Neils Thompson Associate Professor, University of Texas, Austin, Texas, USA

<sup>2</sup> Graduate Research Assistant, University of Texas, Austin, Texas, USA

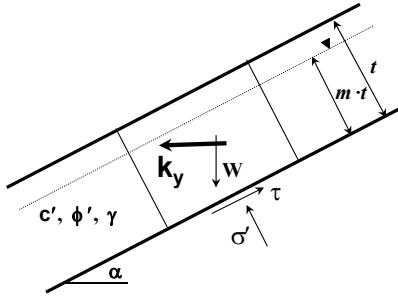


**Figure 1. Infinite slope conditions to calculate  $k_y$**

The level of displacement computed for a given value of  $k_y$  is significantly affected by various characteristics of the acceleration-time history. To assess the range of potential displacements, displacements are computed for a suite of potential acceleration-time histories. Alternatively, empirical predictive models for sliding displacement, which have been developed based on large databases of ground motions [e.g., 5], can be used to estimate the sliding displacement based on  $k_y$  and the expected level of ground shaking.

Several sources of uncertainty are present when predicting the expected level of earthquake-induced sliding displacement for a slope. The most significant uncertainties include: (1) the intensity and characteristics of ground shaking, (2) the computed displacement given the intensity of shaking, and (3) the soil properties used to compute  $k_y$ . Current practice acknowledges these uncertainties, but does not rigorously incorporate them into the assessment of sliding displacement. Rathje and Saygili [6, 7] presented a probabilistic framework for sliding displacement that addresses uncertainties in ground motion and sliding displacement predictions. This paper extends that work in several ways. Improved displacement models are developed, the framework is derived for use with the output from stand alone seismic hazard codes, and an approximation to the probabilistic assessment of vectors of ground motion parameters is evaluated. The probabilistic framework is applied to a site in Northern California and comparisons are made with previous approaches. Additionally, we present a framework to address the uncertainties in soil properties and evaluate their influence on the displacement hazard.

### HAZARD ASSESSMENT

A probabilistic assessment of sliding displacement ( $D$ ) provides a displacement hazard curve, which is a plot of the mean annual rate of exceedance ( $\lambda_D$ ) for different levels of displacement [7]. If  $D$  can be represented as a function of a single ground motion parameter ( $GM$ ), the mean annual rate of exceedance for a displacement level  $x$  is defined as:

$$\lambda_D(x) = \sum_i P[D > x | GM_i] \cdot P[GM_i] \quad (3)$$

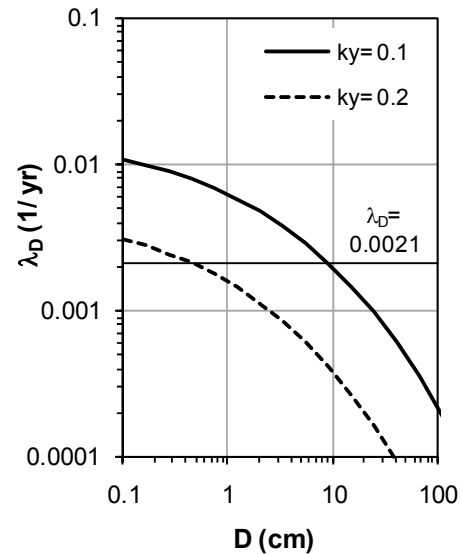
where  $P[D > x | GM_i]$  represents the probability the displacement level  $x$  is exceeded when the ground motion level is equal to  $GM_i$ , and  $P[GM_i]$  is the annual probability of occurrence of ground motion level  $GM_i$ . The first term in equation (3) is derived from a displacement predictive model and its standard deviation, while the second term is derived from the ground motion hazard curve for  $GM$ . The sum in equation (3) represents integration over all possible ground motion levels. Because only a single ground motion parameter is used to predict  $D$ , this approach is considered a scalar probabilistic seismic hazard assessment (PSHA).

Figure 2 displays example hazard curves for sliding displacement derived from equation (3) using a hypothetical ground motion hazard curve and two different values of  $k_y$ . The displacement curves represent the mean annual rate of exceedance ( $\lambda_D$ ) for levels of displacement ranging from 0.1 cm to 100 cm. Similar to ground motion hazard curves, larger displacement levels are less likely (smaller  $\lambda_D$ ) than smaller displacements. The yield acceleration significantly influences the displacement hazard curves. For example, the displacement with a 10% probability of exceedance in 50 years (i.e.,  $\lambda_D = 0.0021$  1/yr) is 9 cm for  $k_y = 0.1$  g and 0.5 cm for  $k_y = 0.2$  g. At this hazard level, the difference is more than an order of magnitude.

Equation (3) assumes that the displacement predictive model is sufficient [8]; i.e., the model sufficiently predicts displacement in terms of  $GM$  without the need for specifying the earthquake magnitude or site-to-source distance. As developed in the next section, when using a single ground motion parameter to predict  $D$ , displacements vary with earthquake magnitude. In this case, equation (3) must be modified to [9]:

$$\lambda_D(x) = \sum_i \sum_j P[D > x | GM_i, M_j] \cdot P[M_j | GM_i] \cdot P[GM_i] \quad (4)$$

where  $P[D > x | GM_i, M_j]$  represents the probability of  $D > x$  given a ground motion level  $GM_i$  and an earthquake magnitude  $M_j$ , and  $P[M_j | GM_i]$  is the probability of occurrence of  $M_j$  given ground motion level  $GM_i$ . This information regarding  $P[M_j | GM_i]$  can be derived from the hazard deaggregation for  $GM$ . The double summation in equation (4) represents integration over all ground motion levels and all earthquake magnitudes.



**Figure 2. Example hazard curve for sliding displacement for different values of yield acceleration.**

If the sliding displacement is a function of two ground motion parameters ( $GM1$  and  $GM2$ ), then a vector PSHA (VPSHA) is required and equation (3) is modified to [10, 11]:

$$\lambda_D(x) = \sum_i \sum_k P[D > x | GM1_i, GM2_k] \cdot P[GM1_i, GM2_k] \quad (5)$$

where  $P[D > x | GM1_i, GM2_k]$  represents the probability of  $D > x$  given the joint occurrence of ground motion levels  $GM1_i$  and  $GM2_k$ , and  $P[GM1_i, GM2_k]$  is the joint annual probability of occurrence of ground motion levels  $GM1_i$  and  $GM2_k$ . This joint annual probability of occurrence is computed via a vector PSHA for the ground motion hazard [7, 10]. This analysis requires a specialized PSHA code, ground motion prediction equations for the two ground motion parameters, and the correlation coefficient ( $\rho$ ) between the two ground motion parameters. The double summation in equation (5) represents integration over all ground motion levels for ground motion parameters  $GM1$  and  $GM2$ .

Figure 3 displays typical scalar ground motion hazard information derived from PSHA for the ground motion parameter peak ground acceleration (PGA). The familiar hazard curve, which plots the mean annual rate of exceedance ( $\lambda_{GM}$ ) versus ground motion level, is shown in Figure 3(a) for a hypothetical example. This scalar hazard curve indicates that the PGA level with a 10% probability of exceedance in 50 years ( $\lambda_{GM} = 0.0021$  1/yr) is about 0.5 g and the PGA level with a 2% probability of exceedance in 50 years ( $\lambda_{GM} = 0.0004$  1/yr) is about 0.8 g.

To develop the displacement hazard for a site (equation 3), the discrete annual probabilities of occurrence, not exceedance, of different ground motions levels are required. This information represents a probability mass function and can be derived from the output from a PSHA code using:

$$P[GM_i] = \frac{\lambda_{GM,i} + \lambda_{GM,i-1}}{2} - \frac{\lambda_{GM,i} + \lambda_{GM,i+1}}{2} = \frac{\lambda_{GM,i-1} - \lambda_{GM,i+1}}{2} \quad (6)$$

where  $\lambda_{GM,i-1}$ ,  $\lambda_{GM,i}$ , and  $\lambda_{GM,i+1}$  represent adjacent hazard values centred about ground motion level  $GM_i$ . Figure 3(b) plots discrete values of annual probability of occurrence for PGA based on the hazard curve shown in Figure 3(a). The smallest values of PGA have the largest probability of occurrence, but also represent the least damaging motions. Note that the discrete probabilities are a function of the size of the ground motion bins (e.g., difference between successive PGA values in a hazard curve), and thus the bin size should be displayed in the plot of discrete probabilities. In PSHA, the bin size generally increases with increasing level of ground motion [12], and this bin representation is used in Figure 3(b). An alternative description of the ground motion probabilities that is not affected by bin size is the mean rate density function [7, 10], which is analogous to a probability density function.

For vector PSHA, specialized PSHA software is required that computes the joint annual probability of occurrence of pairs of ground motion parameters,  $P[GM1_i, GM2_k]$ . Vector PSHA codes for this purpose have been developed by Dr. Norman Abrahamson [13] and Dr. Paolo Bazzurro [14], but no commercially available code exists at this time. The general methodology for computing the vector hazard has been outlined by Bazzurro and Cornell [10].

Alternatively,  $P[GM1_i, GM2_k]$  can be approximated from the scalar hazard curve for  $GM1$  and additional information, including the deaggregation of the hazard for  $GM1$ , a predictive relationship for  $GM2$ , and the correlation coefficient ( $\rho$ ) between  $GM1$  and  $GM2$  [12]. This approximation is based on the conditional probability of  $GM2$  given a value of  $GM1$ , and the probability of occurrence of  $GM1$  [12]:

$$P[GM1_i, GM2_k] = P[GM2_k | GM1_i] \cdot P[GM1_i] = \left( \sum_j \sum_n P[GM2_k | GM1_i, M_j, R_n] \cdot P[M_j, R_n] \right) \cdot P[GM1_i]$$

In the expanded expression in (7),  $P[GM1_i]$  is the probability of occurrence of  $GM1$ ,  $P[M_j, R_n]$  represents the probability of occurrence of different earthquake magnitude ( $M$ ) and distance ( $R$ ) pairs, and  $P[GM2_k | GM1_i, M_j, R_n]$  is the probability of  $GM2$  conditional on ground motion level  $GM1_i$  and the earthquake scenario  $M_j, R_n$ . The double summation in equation (7) represents integration over all earthquake magnitudes and all distances.  $P[GM1_i]$  can be derived from the scalar hazard curve of  $GM1$  using (6),  $P[M_j, R_n]$  comes from the deaggregation of the hazard of  $GM1$ , and  $P[GM2_k | GM1_i, M_j, R_n]$  can be derived from ground motion prediction relationships for  $GM1$  and  $GM2$  along with the correlation coefficient between  $GM1$  and  $GM2$ . The required expressions to compute  $P[GM2_k | GM1_i, M_j, R_n]$  are given in Bazzurro and Cornell [10] and Rathje and Saygili [7]. Equation (7) allows one to develop the VPSHA information using the results of scalar PSHA, rather than developing a full VPSHA code.

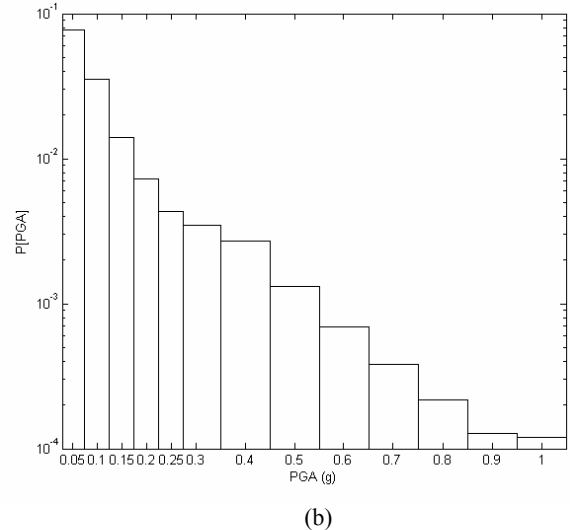
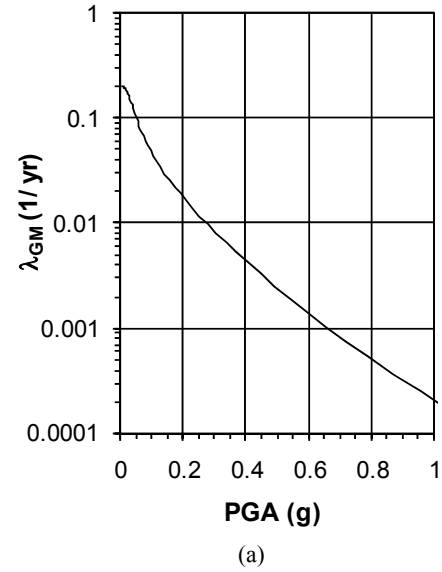
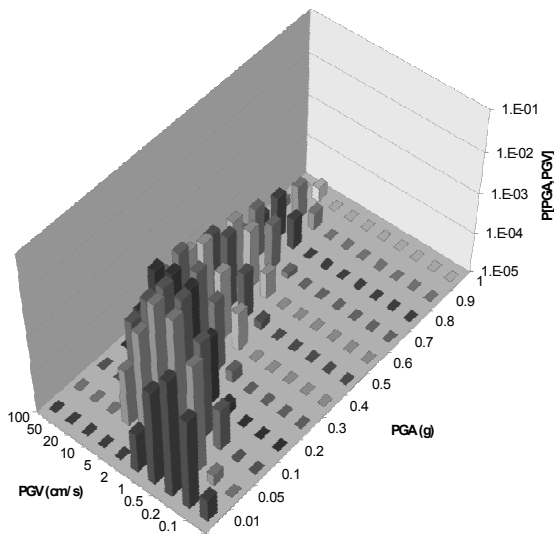


Figure 3. (a) Hazard curve and (b) annual probability of occurrence for PGA from scalar PSHA.



**Figure 4. Joint annual probabilities of occurrence for PGA-PGV pairs**

The vector hazard approximation in (7) theoretically is only valid for situations where a single ground motion prediction equation was used to derive the scalar hazard curve for  $GMI$  [12]. In cases where the scalar hazard curve incorporates epistemic uncertainty via logic trees and multiple ground motion prediction relationships, the joint hazard can be computed using each predictive relationship and the results combined via a weighting scheme [12].

Figure 4 displays discrete values of joint annual probability of occurrence,  $P[GMI, GM2]$ , for  $GMI = PGA$  and  $GM2 = PGV$  (peak ground velocity) for the same hypothetical example from Figure 3 and  $\rho$  equal to 0.6. These values were computed using the VPSHA code developed by Abrahamson (personal communication). In Figure 4, pairs of smaller values of (PGA, PGV) have larger probabilities of occurrence, while pairs of larger values of (PGA, PGV) have smaller probabilities. Also, notice that the probability of a small value of PGA occurring with a large value of PGV (and vice versa) is essentially zero. This result is due to the relationship between ground motion parameters derived from the same acceleration-time history, i.e., it is virtually impossible for a motion with  $PGA = 0.01$  g to also have  $PGV = 100$  cm/s. The correlation coefficient used to derive the vector hazard can significantly affect the ground motion hazard levels and subsequent displacement hazard curve. The appropriate value of  $\rho$  depends on the ground motion parameters under consideration and must be derived from large ground motion databases. Baker [15], Rathje and Saygili [7], and Baker and Jayaram [16] provide estimates of  $\rho$  for different pairs of ground motion parameters.

After specifying the ground motion hazard in terms of a scalar or vector of ground motion parameters (e.g., Figures 3, 4), the only remaining information required to develop a displacement hazard curve is a displacement predictive model. These models are used to compute the displacement probabilities in equations (3) through (5), and are discussed in the next section.

#### PREDICTIVE MODELS FOR DISPLACEMENT

The computation of a displacement hazard curve requires a predictive model for the sliding displacement in terms of one or more ground motion parameters (equations 3 through 5). Saygili and Rathje [17] provide displacement predictive models appropriate for scalar and vector hazard analyses.

These models are described next, and the original scalar model is modified and improved to deal with the issue of sufficiency.

The empirical displacement models are based on rigid sliding block displacements computed from recorded horizontal acceleration-time histories. Over 2,000 motions were used, and each was scaled by scale factors of 1.0, 2.0 and 3.0. Displacements were calculated for  $k_y$  values of 0.05, 0.1, 0.2, and 0.3, and the resulting displacement data set encompassed over 14,000 non-zero displacements.

The scalar model presented by Saygili and Rathje [17] predicts sliding displacement based on the parameters PGA and  $k_y$ . This model displayed large variability, with a standard deviation in natural log space ( $\sigma_{ln}$ ) of 1.13. Additionally, the mean residuals (residual =  $\ln(\text{observed}) - \ln(\text{predicted})$ ) for this relationship displayed an increasing trend with increasing earthquake magnitude (Figure 5(a)), indicating that the ground motion parameter PGA was not sufficient to provide an unbiased estimate of displacement without also specifying earthquake magnitude. This regression criterion was defined as the sufficiency criterion by Cornell and Luco [8]. The residuals in Figure 5(a) also indicate that the original (PGA) model tends to overpredict displacements for small magnitude events and underpredict displacements for large magnitude events. As large magnitude earthquakes represent most design events, the original scalar (PGA) model is unconservative. The mean residuals for the scalar models do not vary with distance, indicating that the models are sufficient with respect to distance.

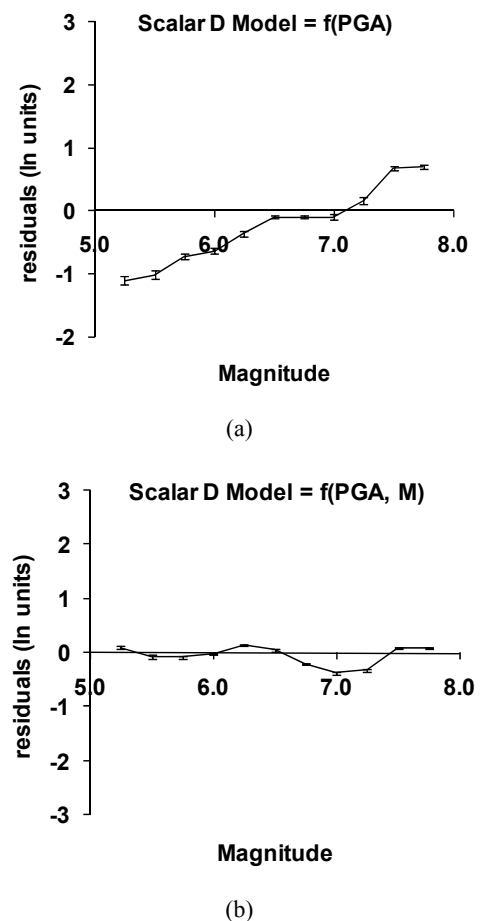


**Figure 5. Mean residuals versus earthquake magnitude for (a) the scalar D model using PGA, and (b) the scalar D model using PGA and M.**

To address the sufficiency issue, a modified scalar model for displacement in terms of PGA, M, and  $k_y$  is proposed.

$$\ln D = a_1 + a_2 \left( \frac{k_y}{PGA} \right) + a_3 \left( \frac{k_y}{PGA} \right)^2 + a_4 \left( \frac{k_y}{PGA} \right)^3 + a_5 \left( \frac{k_y}{PGA} \right)^4 + a_6 \ln(PGA) + a_7 (M - 6) \quad (8)$$

where  $D$  is in units of cm,  $k_y$  and PGA are in units of g, and  $M$  is moment magnitude. The coefficients for the scalar (PGA, M) model are given in Table 1.

**Table 1. Model parameters for scalar and vector models for sliding displacement**

Parameter	Scalar Model (PGA, M)	Vector Model (PGA, PGV)
$a_1$	4.89	-1.56
$a_2$	-4.85	-4.58
$a_3$	-19.64	-20.84
$a_4$	42.49	44.75
$a_5$	-29.06	-30.50
$a_6$	0.72	-0.64
$a_7$	0.89	1.55

The overall standard deviation for the scalar (PGA, M) model is 0.95, an improvement over the (PGA) scalar model ( $\sigma_{ln} = 1.13$ ). However, the standard deviation was observed to vary with  $k_y / PGA$  (Figure 6), similar to the results from Saygili and Rathje [17]. Compared with the scalar (PGA) model, the scalar (PGA, M) model reduces  $\sigma_{ln}$  by 15% to 25%. The standard deviation for the scalar (PGA, M) model can be represented as a second order polynomial:

$$\sigma_{ln} = 0.732 + 0.789 \cdot \frac{k_y}{PGA} - 0.539 \cdot \left( \frac{k_y}{PGA} \right)^2 \quad (9)$$

Generally, the standard deviation varies with  $k_y / PGA$  due to differences in the amount of an acceleration-time history sampled by the displacement calculation. At small values of  $k_y / PGA$  there are many displacement episodes and each episode samples a significant amount of the ground motion. Thus, the information provided by the term  $M$  reduces the standard deviation. At larger values of  $k_y / PGA$  there are few displacement episodes and each episode samples only a small portion of the ground motion. As a result, the addition of the term  $M$  to the predictive model does not provide enough meaningful information to reduce the standard deviation.

The recommended two ground motion parameter vector model for displacement utilizes PGA and PGV and was developed by Saygili and Rathje [17]. The form of this model is:

$$\ln D = a_1 + a_2 \left( \frac{k_y}{PGA} \right) + a_3 \left( \frac{k_y}{PGA} \right)^2 + a_4 \left( \frac{k_y}{PGA} \right)^3 + a_5 \left( \frac{k_y}{PGA} \right)^4 + a_6 \ln(PGA) + a_7 \ln(PGV) \quad (10)$$

where PGV is in units of cm/s and the model coefficients are given in Table 1. The resulting standard deviation varies significantly with  $k_y / PGA$  (Figure 6) due to the fact that PGV

provides important information about the ground motion in terms of the displacement potential. This observation is valid particularly at small values of  $k_y / PGA$ , where the standard deviation is reduced by as much as 50%. The standard deviation for the vector (PGA, PGV) model of displacement can be represented as a first order polynomial [17]:

$$\sigma_{ln} = 0.405 + 0.524 \cdot \frac{k_y}{PGA} \quad (11)$$

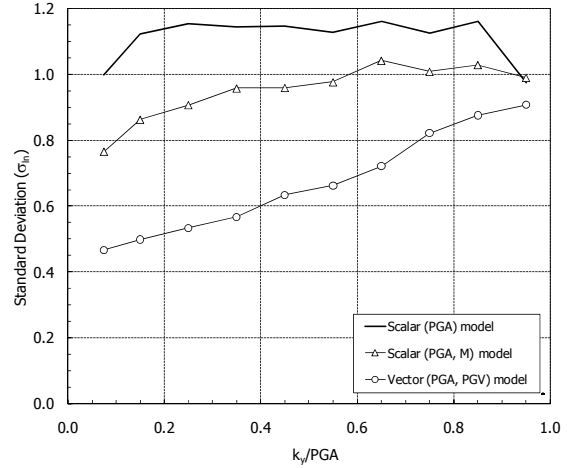


**Figure 6. Variation of standard deviation with  $k_y/PGA$  for different displacement models.**

Figure 7(a) compares the previous scalar displacement model from [17], and the modified version developed here for  $PGA=0.33$  g. The (PGA) scalar model predicts displacements that range from 40 to 0.5 cm for the  $k_y$  values considered. The (PGA, M) model demonstrates the important information provided by earthquake magnitude. For the same PGA, the (PGA, M) model predicts larger displacements as earthquake magnitude increases. The difference in the predicted displacements for  $M = 5.5$  and  $7.5$  is larger than a factor of 5.0. Magnitude has a significant impact on the predicted displacement because the frequency content and duration of shaking is magnitude dependent. Figure 7(b) provides a comparison between the median displacements predicted by the scalar (PGA) model, the scalar (PGA, M) model and the vector (PGA, PGV) model for a specific scenario:  $M = 7$ ,  $R = 5$  km, rock site conditions, and a strike-slip faulting. The values of PGA and PGV used to predict displacement are 0.33 g and 30 cm/s, respectively, and these values are the median values from the Boore and Atkinson [18] ground motion prediction relationship. The results in Figure 7(b) indicate that the (PGA, PGV) model predicts displacements about 40% smaller than the (PGA, M) model and 30% smaller than the (PGA) model for the  $k_y$  values shown. Considering other earthquake magnitude and distance scenarios, the (PGA, PGV) model consistently predicts displacements 30 to 50% smaller than the (PGA, M) model. This significant difference is due to the strong influence of PGV on the level of displacement, and the fact that this information is not fully taken into account when using the (PGA, M) model.

The quantitative comparison between the (PGA, M) and (PGA, PGV) models in terms of regression parameters (i.e., standard deviation, bias, etc.) indicates that the vector (PGA, PGV) model is the superior model. The (PGA) model should not be used because it is unconservative for large magnitude earthquakes. The (PGA, PGV) model is also an attractive model from an evaluation perspective because it predicts smaller displacements. However, none of these models has been validated against field observations of earthquake-

induced landslide occurrence and associated ground motion recordings; thus the accuracy of these models related to field performance is unknown.

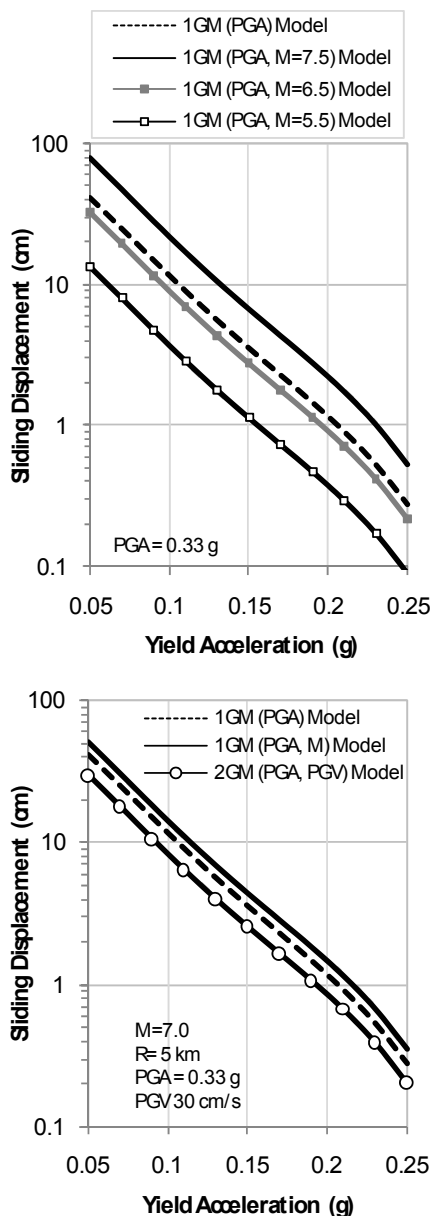


Figure 7. (a) Comparison of scalar displacement models, (b) comparison of scalar and vector displacement models.

#### APPLICATION TO SITE IN NORTHERN CALIFORNIA

To demonstrate the probabilistic procedure for sliding displacement, a hypothetical landslide site was considered in Northern California (37.329N, 122.138 W) in the hills west of the city of San Jose (Figure 8). Potential landslides will be considered with  $k_y$  values between 0.1 g and 0.2 g.

The ground motion hazard was computed using the fault system representation provided by Abrahamson [13], and includes 12 faults within 100 km of the site (Figure 8). The ground motion hazard for PGA was computed using the scalar PSHA code developed by Abrahamson [13] and the Boore and Atkinson [18] ground motion prediction equation. The resulting hazard curve is shown in Figure 9(a). The hazard is significant at this site, with the PGA equal to 0.57 g at  $\lambda_{GM} = 0.0021$  1/yr (i.e., 10% probability of exceedance in 50 years)

and equal to 1.02 g at  $\lambda_{GM} = 0.0004$  1/yr (i.e., 2% probability of exceedance in 50 years).

To utilize the ground motion hazard to develop a displacement hazard curve using the scalar approach (equation 4), the probability of occurrence of different ground motion levels must be computed using equation (6). Figure 9(b) displays the probability of occurrence values derived from the hazard curve in Figure 9(a) using PGA bins ranging in size from 0.05 g to 0.1 g. The other piece of information required for the scalar approach is the magnitude deaggregation for each ground motion level. Figure 9(c) represents the magnitude/distance deaggregation of the PGA hazard for  $\lambda_{GM} = 0.0021$  1/yr. The displacement hazard computation requires only the probability of occurrence of different magnitudes; thus only the magnitude deaggregation is required. Using the data shown in Figure 9(c), the probability of occurrence for each magnitude bin is computed by summing up the values for all distances within the magnitude bin. At this hazard level, the hazard is dominated by events with magnitudes greater than 6.5 and the probability of occurrence within the four largest magnitude bins ( $M = 6.5-7.0, 7.0-7.5, 7.5-8.0, 8.0-8.4$ ) are 0.19, 0.44, 0.18, and 0.12, respectively. This magnitude deaggregation information is derived for each PGA bin used in the analysis (i.e., those shown in Figure 9(b)). For the site analysed here, the magnitude deaggregation did not vary significantly between hazard levels because of the proximity of the site to the San Andreas fault (Figure 8).

Using the scalar hazard information in Figure 9(b) and the magnitude deaggregation information for each hazard level for PGA (e.g., Figure 9(c)), displacement hazard curves were developed using the scalar (PGA) and (PGA, M) models for displacement. Displacement hazard curves for  $k_y = 0.1$  g are shown in Figure 10. For this example, the (PGA, M) model predicts larger displacements than the (PGA) model for each hazard level. The (PGA) model underpredicts the hazard because earthquake magnitudes between 7.0 and 8.0 dominate the hazard (Figure 9(c)) and the (PGA) model underpredicts displacement in this magnitude range (Figure 5). The displacement hazard curves can be used to evaluate the displacement levels for different return periods / hazard levels (i.e.,  $\lambda_D$  values). For the curves shown, the 475 year return period ( $\lambda_D = 0.0021$  1/yr) and 2,475 year return period ( $\lambda_D = 0.0004$  1/yr) displacement levels for the (PGA, M) model are 62 cm and 312 cm, respectively. For the (PGA) model, the displacements at these hazard levels are 30 to 35% smaller.

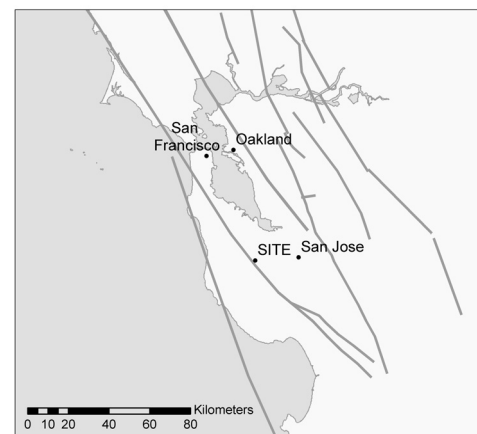


Figure 8. Site location map with faults.

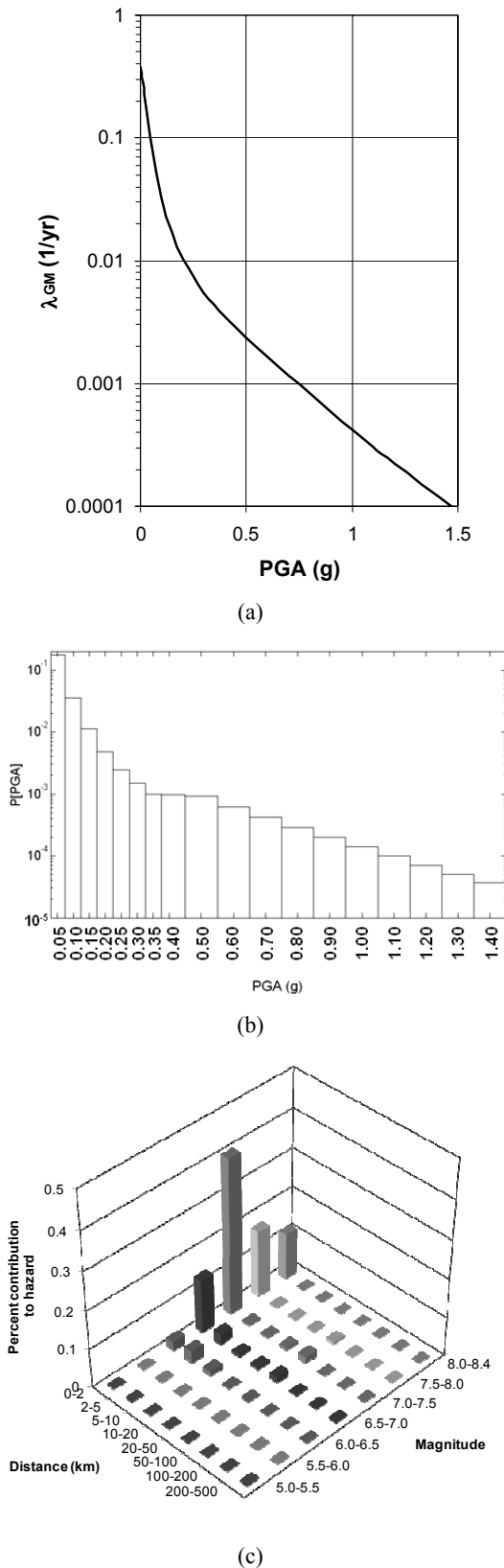


Figure 9. (a) Scalar PGA hazard curve, (b) annual probability of occurrence for each PGA level, and (c) deaggregation of PGA hazard at  $\lambda_{GM} = 0.0021$ .

In current practice, engineers generally use a ground motion for a specific hazard level in a displacement analysis and assume, implicitly, that the computed displacement represents the same level of hazard as the ground motion. However, generally this assumption is not valid. For example, using the 475 year PGA level (0.57 g, Figure 9(a)) and the mean magnitude from the magnitude deaggregation (M 7.3), the median displacement computed for  $k_y = 0.1$  g using the (PGA, M),

(M) model in equation (8) is 80.5 cm. This value is 30% larger than the value of 62 cm from the displacement hazard curve. Using the 2,475 year PGA level (1.02 g, Figure 9(a)) and the mean magnitude from the magnitude deaggregation (M 7.3), the median displacement computed for  $k_y = 0.1$  g using the (PGA, M) model is 229 cm, as opposed to the value of 312 cm derived from the displacement hazard curve. For this long return period, the displacement hazard curve produces a significantly larger displacement because it includes the uncertainty in the displacement prediction.

The vector hazard for the site for the ground motion parameter vector (PGA, PGV) was computed using the vector PSHA code developed by Abrahamson (personal communication). The only additional information required for vector PSHA beyond that required for scalar PSHA is the ground motion prediction relationship for the second ground motion parameter and the correlation coefficient between the two ground motion parameters. For the ground motion parameter vector (PGA, PGV), the Boore and Atkinson [18] ground motion model was used for both parameters and the correlation coefficient was taken as 0.6 based on Rathje and Saygili [7].

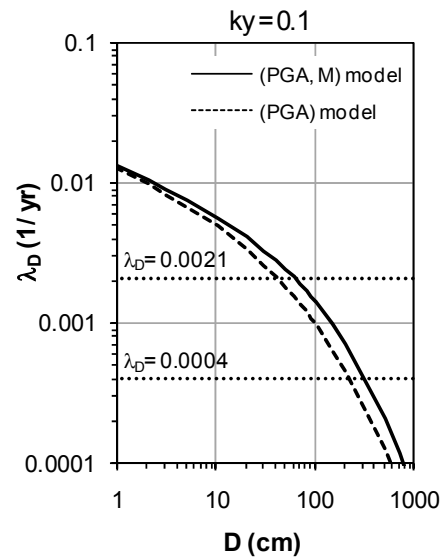


Figure 10. Displacement hazard curves for  $k_y = 0.1$  using the (PGA) and (PGA, M) displacement models.

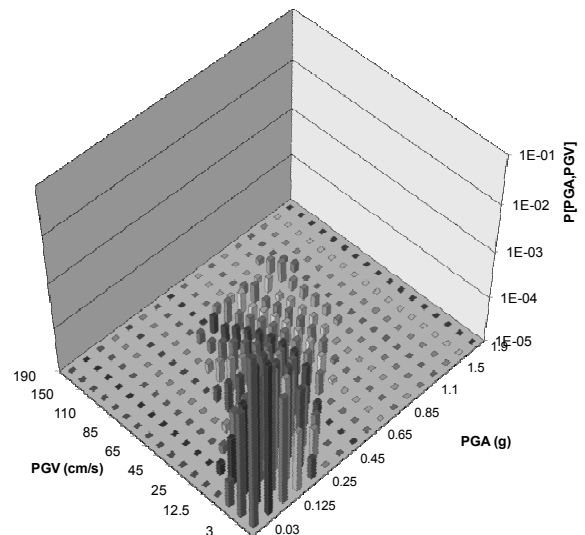
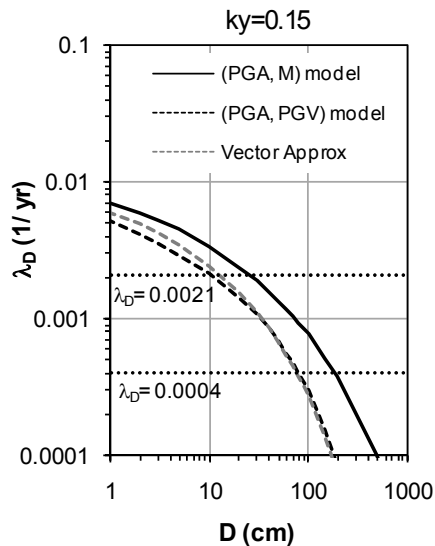


Figure 11. Joint annual probabilities of occurrence for PGA-PGV pairs.



**Figure 12. Displacement hazard curves using scalar (PGA, M) and, vector (PGA, PGV) displacement models for  $k_y = 0.15$ . Vector approximation uses equation (7) to approximate vector ground motion hazard.**

The resulting joint annual probabilities of occurrence for PGA-PGV pairs are shown in Figure 11. Pairs of smaller values of PGA-PGV display probabilities on the order of  $1 \times 10^{-2}$ , while pairs of larger values display probabilities around  $1 \times 10^{-5}$ . Generally, the probability of a small PGV being coupled with a large PGA (or vice versa) is low, as seen in Figure 11, because of the correlation between the two ground motion parameters.

A displacement hazard curve for  $k_y = 0.15$  was derived using the vector hazard approach (equation 5), the (PGA, PGV) vector hazard information in Figure 11, and the (PGA, PGV) displacement prediction model. This displacement hazard curve is shown in Figure 12 along with the curve derived using the scalar (PGA, M) model. The displacement hazard curve based on the vector (PGA, PGV) model displays significantly smaller displacement levels than the scalar (PGA, M) model. At a 475 year return period ( $\lambda_D = 0.0021$  1/yr), the scalar (PGA, M) model predicts 25 cm of displacement while the vector model predicts 10 cm. At a 2,475 year return period ( $\lambda_D = 0.0004$  1/yr) the scalar (PGA, M) model predicts 188 cm of displacement while the vector model predicts 80 cm. Generally, the displacement hazard is reduced by more than a factor of two when the vector model is used. The smaller displacement values are the result of two issues. First, the vector model generally predicts smaller displacements than the scalar model for a given earthquake scenario (M, R), as observed in Figure 7. Second, the standard deviation for the vector displacement model is significantly smaller than the standard deviation for the scalar model (Figure 6). These characteristics combine to produce the reduced hazard when using the vector approach.

Figure 12 also includes a displacement hazard curve based on the vector approach in which the vector hazard for PGA-PGV pairs was approximated using equation (7). Equation (7) approximates the joint annual probabilities of occurrence for pairs of ground motion parameters using: (1) the hazard curve and deaggregation from a scalar PSHA for one ground motion parameter, (2) the predictive model for the second ground motion parameter, and (3) the correlation coefficient between the two ground motion parameters. The appeal of equation (7) is that one can approximate the VPSHA information using the results of scalar PSHA, rather than developing a full VPSHA code. The displacement hazard curve from the vector approximation in Figure 12 is very similar to the curve

developed from rigorous VPSHA, particularly at lower hazard levels. This favourable comparison lends credibility to the vector hazard approximation.

### INFLUENCE OF SOIL PROPERTY UNCERTAINTY

In the framework described above, the uncertainties in the properties of the slope (e.g., soil strength properties, slope angle, etc.) have not been taken into account. Utilizing a single value for  $k_y$  for a slope based on best estimates of these properties ignores potentially significant uncertainties in that value and may lead to inaccurate quantification of landslide hazard. This issue is particularly true when applying the probabilistic framework to landslide hazard mapping efforts where soil properties are assigned based on geologic units, and using single estimates of soil properties within an entire geologic unit is unrealistic due to spatial variability.

The variability in  $k_y$  can be quantified via a logic tree approach applied to the input parameters required to compute  $k_y$ . The general approach for logic tree analysis involves specification of discrete values of each input parameter along with corresponding weights that represent the confidence in each value. The logic tree includes a collection of nodes and branches, in which the nodes represent the input parameter under consideration and the branches stemming from each node represent the specified discrete values for that parameter. Weights must be specified for each discrete value at each node. Often a normal distribution is assumed for each node and three branches are adequate to describe the distribution of values. The three branches can be well represented using the 5<sup>th</sup>, 50<sup>th</sup>, and 95<sup>th</sup> percentiles with weights ( $w$ ) of 0.2, 0.6 and 0.2, respectively [19]. In this case the alternatives represent values of each parameter equal to  $-1.6$ -times the standard deviation ( $\sigma$ ), the mean, and  $+1.6\sigma$ .

An example of a logic tree is shown in Figure 13(a) as applied to discrete values of shear strength parameters  $c'$  and  $\phi'$ . Three values of  $\phi'$  are considered ( $22^\circ$ ,  $26^\circ$ , and  $30^\circ$ ), along with three values of  $c'$  (10, 15, and 20 kPa). These values were developed based on mean values of  $\phi' = 26^\circ$  and  $c' = 15$  kPa, along with coefficients of variation ( $COV = \sigma / \text{mean}$ ) equal to 0.1 and 0.2, respectively, for  $\phi'$  and  $c'$  [20]. The other parameters used to compute  $k_y$  are fixed at:  $\alpha = 30^\circ$ ,  $\gamma = 18.8$  kN/m<sup>3</sup>,  $t = 3.0$  m, and  $m = 0$ . A  $k_y$  value is computed for each full branch of the logic tree and the corresponding weight for that value of  $k_y$  is computed from the product of the weights along the entire path of that branch. For this example the  $k_y$  values vary from 0.016 g to 0.3 g, a significant range. The  $k_y$  that is computed from the best estimate (or mean) values of  $c'$  and  $\phi'$  (15 kPa and  $26^\circ$ , respectively) is 0.16 and this value has the largest weight in the logic tree (Figure 13(a)). The variation in  $k_y$  can also be displayed in terms of a probability mass function, as shown in Figure 13(b). In this case, most of the  $k_y$  values are concentrated between 0.1 and 0.2 g.

To incorporate the logic tree for  $k_y$  into the hazard assessment for sliding displacement, a displacement hazard curve is computed for each  $k_y$  value in the logic tree. These hazard curves are all potential realizations of the hazard assessment, but each is associated with a different weight based on the weight corresponding to the value of  $k_y$ . A weighted mean displacement hazard curve is computed using the different hazard curves and their associated weights, in the same way that a mean hazard curve is computed for ground motion parameters in PSHA [e.g., 21].



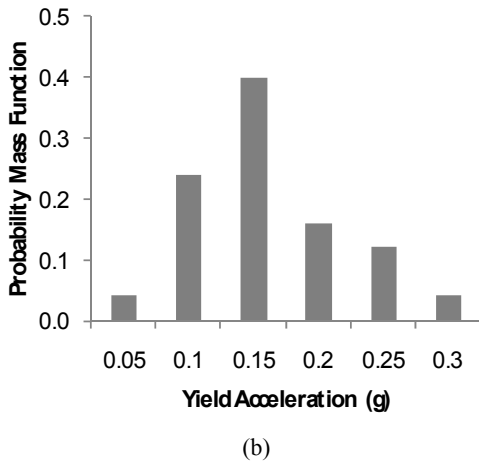
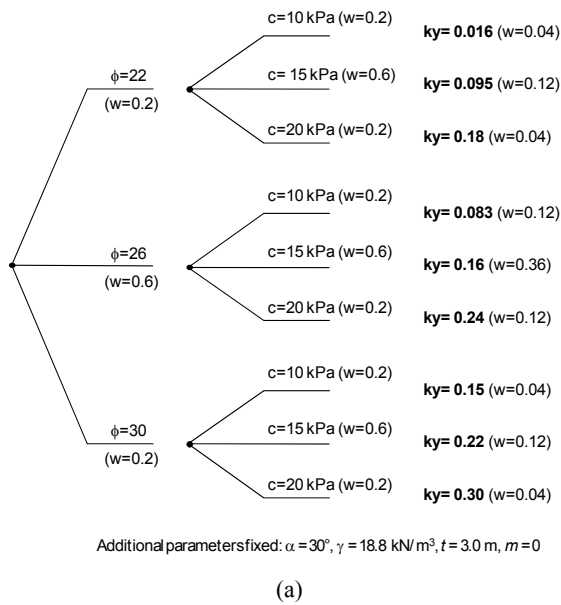


Figure 13. (a) Logic tree for the assessment of yield acceleration, and (b) resulting probability mass function for  $k_y$ .

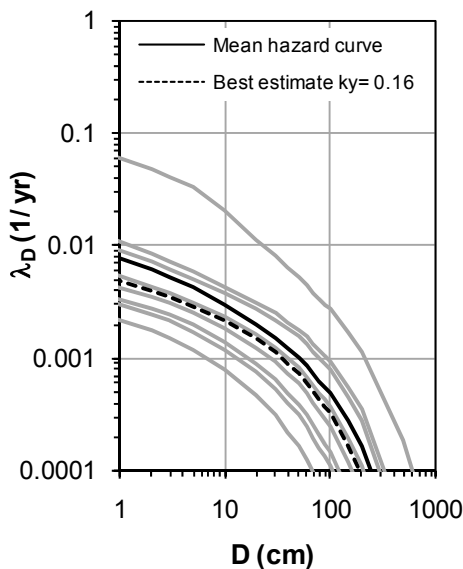


Figure 14. Displacement hazard curves for the logic tree shown in Figure 13.

Figure 14 presents the resulting displacement hazard curves from the logic tree analysis. These displacement hazard curves use the (PGA, PGV) vector model for the displacement and the vector hazard information shown in Figure 11. Nine hazard curves are shown in gray and each represents a curve for single value of  $k_y$  in the logic tree (Figure 13(a)). These hazard curves are weighted based on their corresponding logic tree weights to develop a weighted mean hazard curve. The mean hazard curve indicates that the displacement hazards for 10% probability of exceedance in 50 years and 2% probability of exceedance in 50 years are 18 cm and 115 cm, respectively.

Also shown in Figure 14 for comparison is the hazard curve for  $k_y = 0.16 \text{ g}$ , which represent the yield acceleration associated with the best estimate shear strength properties,  $c' = 15 \text{ kPa}$  and  $\phi' = 26^\circ$ . This hazard curve falls below the mean hazard curve from the logic tree analysis, indicating that ignoring uncertainties in the soil properties leads to unconservative estimates of the displacement hazard. In this case, the hazard curve for  $k_y = 0.16 \text{ g}$  produces displacement hazards of 10 cm and 85 cm at 10% and 2% probabilities of exceedance in 50 years, respectively. These values are about 25% to 45% smaller than the values estimated from the mean hazard curve.

### CONCLUSIONS

This paper presents a probabilistic framework for the assessment of earthquake-induced permanent displacements of slopes. The probabilistic framework accounts for the most significant uncertainties present in the evaluation of permanent displacement of slopes: (1) the intensity and characteristics of ground shaking, (2) the computed displacement given the characteristics of shaking, and (3) the soil properties used to compute the yield acceleration of the slope. Current practice acknowledges these uncertainties, but does not rigorously incorporate them when evaluating the expected level of sliding displacement in slopes.

Incorporating uncertainties in ground motion and sliding displacement prediction is achieved through the development of a displacement hazard curve, which represents the mean annual rate of exceedance for different levels of displacement. This analysis requires the PSHA for the ground motion parameter(s) that are used to predict sliding displacement. A scalar approach, which uses a single ground motion parameter to predict displacement, and a vector approach, which uses two ground motion parameters, were introduced. The advantage of using the vector approach is that incorporating multiple ground motion parameters in the sliding displacement model typically results in less variability in the sliding displacement prediction.

The previously developed scalar displacement model in terms of PGA [17] was modified to include the effects of earthquake magnitude. This (PGA, M) displacement model has a smaller standard deviation than the original (PGA) model, and is the preferred scalar model because it is unbiased relative to earthquake magnitude and distance. Developing a displacement hazard curve using the (PGA, M) displacement model requires a revised hazard equation for displacement that includes magnitude deaggregation information. The vector displacement model uses PGA and PGV to predict sliding displacement.

The scalar and vector approaches were used to develop displacement hazard curves for a site in Northern California. The site was modelled as an infinite slope with shear strength parameters  $c'$  and  $\phi'$ . Scalar and vector PSHA were used to develop hazard and deaggregation information for the required ground motion parameters, and this information was used to develop the displacement hazard curves. For this example, the

displacement hazard was reduced by more than a factor of three when the vector approach was used over the scalar approach. Additionally, it was shown that simply using a ground motion level for a specific hazard level in a displacement analysis does not produce a displacement level with the same hazard level. An approximation method to compute the joint annual probabilities for VPSHA was presented and evaluated. The displacement hazard curve from the VPSHA approximation was similar to that from the rigorous VSPA approach, indicating that the VPSHA approximation provides reasonable results.

Finally, a logic tree approach was proposed to deal with uncertainties in soil properties and their effect on  $k_v$  and the resulting displacement hazard curves. This approach assigns weights to potential values of various soil properties, computes the corresponding values of  $k_v$  and combined weights based on these properties, and calculates a displacement hazard curve for each value of  $k_v$ . These hazard curves are combined using the individual weights to produce a weighted mean hazard curve. For the example shown, the mean hazard curve displays an increased hazard over the displacement hazard curve developed based on the best estimate soil properties. This result illustrates the potential for unconservative estimates of sliding displacement when soil property uncertainties are not taken into account.

#### ACKNOWLEDGMENTS

This work benefited from interactions with Professor Julian Bommer, Dr. Peter Stafford, and Dr. Fleur Strausser at Imperial College London, Dr. Norman Abrahamson of Pacific Gas and Electric, Co, and Dr. Paolo Bazzurro of AIR Worldwide. Financial support was provided by the U.S. Geological Survey (USGS), Department of the Interior, under grants 06HQGR0057 and 08HQGR0024. The views and conclusions contained in this document are those of the authors and should not be interpreted as necessarily representing the official policies, either expressed or implied, of the U.S. Government.

#### REFERENCES

- Jibson, R.W., Harp, E.L. and Michael, J.A., (1998) A method for producing digital probabilistic seismic landslide hazard maps: An example from the Los Angeles California area. *U.S. Geol. Surv. Open-File Rep. 98-113*, 17 pp.
- Bray, J.D. and Rathje, E.M. (1998) "Earthquake-Induced Displacements of Solid-Waste Landfills," *J. of Geotechnical and Geoenvironmental Engineering*, ASCE, 124(3), 242-253.
- Keefer, D.K., (1984) "Landslides caused by earthquakes." *Geol. Soc. Am. Bull.* 95, pp. 406-421.
- McCrink, T.P., (2001) "Mapping earthquake-induced landslide hazards in Santa Cruz County" in Ferriz, H. and Anderson, R., editors, *Engineering geology practice in northern California: California Geological Survey Bulletin 210 / Association of Engineering Geologists Special Publication 12*, p.77-94.
- Jibson, R.W., (2007) "Regression models for estimating coseismic landslide displacement." *Eng. Geol.* 91, 209-218.
- Rathje, E.M. and Saygili, G. (2006) "A Vector Hazard Approach for Newmark Sliding Block Analyses," *Earthquake Geotechnical Engineering Workshop*, University of Canterbury, Christchurch, New Zealand, 20-23 November.
- Rathje, E.M. and Saygili, G. (2008) "Probabilistic Seismic Hazard Analysis for the Sliding Displacement of Slopes: Scalar and Vector Approaches," *Journal of Geotechnical and Geoenvironmental Engineering*, ASCE, 134(6), 804-814.
- Cornell, C. A., and Luco, N., (2001) "Ground motion intensity measures for structural performance assessment at near-fault sites," *Proceedings of the U.S.-Japan joint workshop and third grantees meeting*, U.S.-Japan Coop. Res. on Urban EQ. Disaster Mitigation, Seattle, Washington.
- Luco N. (2002) "Probabilistic Seismic Demand Analysis, SMRF Connection Fractures, and Near-source Effects" Ph.D. Dissertation, Department of Civil and Environmental Engineering, Stanford University, CA.
- Bazzurro, P. and Cornell, C.A. (2002) "Vector-Valued Probabilistic Seismic Hazard Analysis (VPSHA)," *Seventh U.S. National Conference on Earthquake Engineering*, EERI, Vol. II, 1313-1322.
- Baker, J.W. and Cornell, C.A. (2005) "A Vector-Valued Ground Motion Intensity Measure Consisting of Spectral Acceleration and Epsilon." *Earthquake Engineering & Structural Dynamics*, 34 (10), 1193-1217.
- Bazzurro, P. (1998) "Probabilistic Seismic Demand Analysis" Ph.D. Dissertation, Department of Civil and Environmental Engineering, Stanford University, CA.
- Abrahamson, N. (2007) Personal Communication
- Bazzurro, P. (2007) Personal Communication
- Baker, J.W. (2007) "Correlation of ground motion intensity parameters used for predicting structural and geotechnical response," *10th International Conference on Applications of Statistics and Probability in Civil Engineering*, Tokyo, Japan.
- Baker, J.W. and Jayaram, N. (2008) "Correlation of spectral acceleration values from NGA ground motion models" *Earthquake Spectra*, EERI, 24(1), 299-318
- Saygili, G. and Rathje, E.M. (2008) "Empirical Predictive Models for earthquake-Induced Sliding Displacements of Slopes," *Journal of Geotechnical and Geoenvironmental Engineering*, ASCE, 134(6), 790-803.
- Boore, D. M. and Atkinson, G. M. (2008) "Ground-motion Prediction Equations for the Average Horizontal Component of PGA, PGV and 5%-Damped PSA at Spectral Periods between 0.01 s and 10.0 s," *Earthquake Spectra*, EERI, 24(1), 99-138.
- Keefer, D.L. and Bodily S.E. (1983) "Three Point Approximations for Continuous Random Variables." *Management Science*, 595-609.
- Jones, A.L., Kramer, S.L. and Arduino, P. (2002) "Estimation of uncertainty in geotechnical properties for performance-based earthquake engineering." *PEER Report 2002/16*, Pacific Earthquake Engineering Research Center, University of California, Berkeley.
- Bommer, J.J., Scherbaum, F., Bungum, H., Cotton, F., Sabetta, F., and Abrahamson, N.A. (2005) "On the Use of Logic Trees for Ground-Motion Prediction Equations in Seismic-Hazard Analysis." *Bulletin of the Seismological Society of America*, 95(2), 377-389.